Chinese Chemical Letters 37 (2026) 111641

Contents lists available at ScienceDirect

Chinese Chemical Letters

journal homepage: www.elsevier.com/locate/cclet

Carbon monoxide-engineered M2 exosomes enhance osteoimmunology and promote alveolar bone regeneration

Zhiyuan Shen[a,b], Tianyi Li[a,b], Zijie Zhang[a,b], Jiani Liu[a,b], Jun Wu[c,d,*], Qing Li[a,b,*], Fulan Wei[a,b,*]

[a] Department of Orthodontics & Oral and Maxillofacial Surgery & Pediatric Dentistry, School and Hospital of Stomatology, Cheeloo College of Medicine, Shandong University, Ji'nan 250012, China
[b] Shandong Key Laboratory of Oral Tissue Regeneration & Shandong Engineering Research Center of Dental Materials and Oral Tissue Regeneration & Shandong Provincial Clinical Research Center for Oral Diseases, Ji'nan 250012, China
[c] Bioscience and Biomedical Engineering Thrust, The Hong Kong University of Science and Technology (Guangzhou), Nansha, Guangzhou 511400, China
[d] Division of Life Science, The Hong Kong University of Science and Technology, Hong Kong SAR 999077, China

ARTICLE INFO

Article history:
Received 6 May 2025
Revised 20 July 2025
Accepted 25 July 2025
Available online 26 July 2025

Keywords:
CO-M2-Exos
Carbon monoxide
Osteogenesis
miRNA-21
Lhx8
Alveolar bone

ABSTRACT

Macrophage-derived exosomes have demonstrated considerable potential for promoting bone regeneration. This study proposes a novel engineered therapeutic strategy that utilizes carbon monoxide releasing prodrugs (TG-Fe CORMs) to selectively induce M2 macrophage polarization, thereby enhancing the production of M2 macrophage-derived exosomes (CO-M2-Exos). These exosomes have been observed to significantly promote osteogenesis and accelerate alveolar bone regeneration through the microRNA-21/Lhx8 signaling pathway. Notably, these exosomes possess several advantageous characteristics, including their capacity for remarkable regenerative effects, low immunogenicity, and high cellular uptake, which renders them promising cell-free therapy for addressing alveolar bone defects. Moreover, the scalable production of CO-M2-Exos successfully overcomes the significant challenges associated with traditional exosome-based therapies, such as the complexity of cell culture processes, the instability of phenotype, and the low yield of exosome production. This engineered approach offers a reliable, efficient, and cost-effective solution for clinical translation, particularly for promoting alveolar bone regeneration in cases of severe bone atrophy following tooth extraction.

© 2026 Published by Elsevier B.V. on behalf of Chinese Chemical Society and Institute of Materia Medica, Chinese Academy of Medical Sciences.

In dentistry, the study of alveolar bone regeneration is paramount due to its critical role in providing stable support for teeth [1,2]. The alveolar bone typically maintains a dynamic balance between resorption and regeneration, which is crucial for bone health [3,4]. However, surgical procedures such as tooth extraction can disrupt dynamic balance, leading to excessive absorption of alveolar bone and bone atrophy [5,6], seriously affecting oral health and aesthetic effects [7,8]. To prevent severe bone atrophy after tooth extraction, clinical treatment methods such as site preservation and GBR are used after tooth extraction, but the effect is limited [9]. Using stem cells, growth factors, and scaffolds, tissue engineering emerges as a potential avenue for improving alveolar bone regeneration [10,11]. Yet, this approach faces challenges such as the limited availability of donor cells, the risk of immune rejection, and concerns about the duration and cost of treatments [12].

Macrophages play a critical role in alveolar bone remodeling, with M1 macrophages driving resorption and M2 macrophages promoting regeneration [13,14]. While pro-inflammatory M1 macrophages are implicated in bone resorption during inflammation, anti-inflammatory M2 macrophages aid bone regeneration [15,16]. However, the inefficiencies and adverse effects of traditional induction methods hinder the effective use of M2 macrophages in alveolar bone regeneration [17–20]. Advancements in the direct application of M2 macrophages are needed to address labor-intensive cell cultures, phenotype instability, and low survival rates post-transplantation [21]. Studies have confirmed that exosomes are not only a natural information carrier, but also an effective platform for regulating information transmission in the process of alveolar bone regeneration [22]. Exosomes have low immunogenicity, high cellular uptake efficiency, and good biocompatibility, which can ensure intercellular communication and maintain *in vivo* balance [23]. Exosomes secreted from different sources have a significant contribution to bone regeneration [24–26], offering an advantageous alternative to conventional cell

* Corresponding authors.
E-mail addresses: junwuhkust@ust.hk (J. Wu), lq580202@sdu.edu.cn (Q. Li), weifl@email.sdu.edu.cn (F. Wei).

https://doi.org/10.1016/j.cclet.2025.111641
1001-8417/© 2026 Published by Elsevier B.V. on behalf of Chinese Chemical Society and Institute of Materia Medica, Chinese Academy of Medical Sciences.

therapy by avoiding its limitations. In particular, exosomes derived from M2 macrophages offer a feasible strategy for alveolar bone regeneration, although the underlying mechanisms require further exploration [27,28].

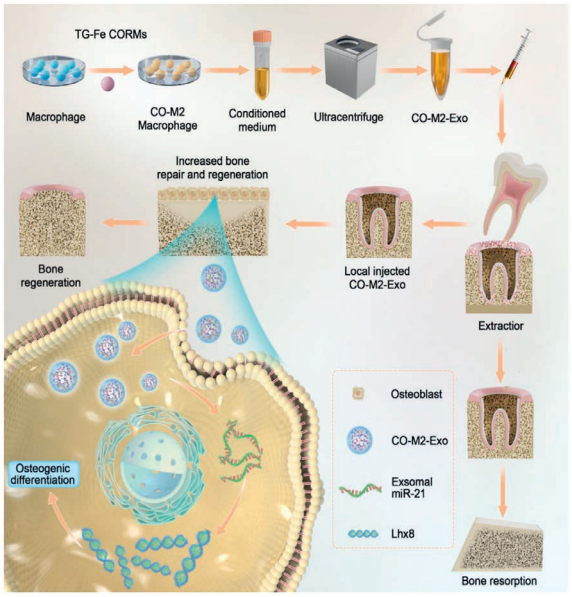
Carbon monoxide (CO), a gaseous signaling molecule, intricately modulates immune responses and inflammation by facilitating M2 macrophage polarization *via* the JAK1/STAT6 pathway [29,30]. Despite its potential, the dual nature of CO in inhibiting cellular functions and inducing apoptosis requires meticulous dosage control. While CO may regulate local immune responses to encourage osteogenic differentiation, ensuring its safe and productive use without adverse effects remains a subject for further research [31]. To address this, we utilized TG-Fe CO-releasing molecules (CORMs), a novel hydrophilic prodrug, enabling precise and controlled delivery of CO to efficiently induce M2 macrophages and produce engineered exosomes (CO-M2-Exos) tailored for therapeutic use. This innovation represents a pioneering approach to leveraging CO for engineering exosomes as a cell-free therapeutic strategy in alveolar bone regeneration.

In this study, we first-ever used carbon monoxide as an innovative tool to modulate immune responses and prevent alveolar bone resorption in post-extraction socket reconstruction. Using hydrophilic TG-Fe CO-releasing molecules (CORMs) [32,33], we induced reparative M2 macrophages to produce CO-M2-Exos with low immunogenicity and high cellular uptake efficiency, providing a pioneering cell-free therapeutic strategy for bone regeneration. These exosomes demonstrated the ability to significantly enhance osteogenesis *via* the previously unexplored miRNA-21/Lhx8 signaling pathway, providing a novel theoretical basis for immune-regulated prevention of alveolar bone atrophy (Scheme 1). The efficient and scalable production of CO-M2-Exos highlights their potential for clinical translation, addressing critical challenges in alveolar bone defect repair and introducing a transformative solution for maintaining alveolar bone volume and promoting regeneration after tooth extraction.

CO is recognized as a potent anti-inflammatory gaseous transmitter molecule, which have received increasing attention for potential therapeutic application [34]. Unfortunately, CO is also a highly toxic gas due to its high binding ability with hemoglobin and myoglobin (Mb) [35]. Accurate control of CO release is one of the key factors for effective therapeutic applications [36]. CO-releasing molecules (CORMs) have been used to simulate the therapeutic effects of CO under several biological conditions [37]. TG-Fe CORMs ($Fe_2\{\mu\text{-}SCH_2CH(OH)CH_2(OH)\}_2(CO)_6$) was obtained using the method described in previous report [38] and the ^{1}H NMR spectra demonstrated the successful synthesis (Fig. S1 in Supporting information). ^{1}H NMR (DMSO–d_6): 5.13 (1H, d, J = 6.0 Hz, ^{ae}CHO*H*), 4.94 (1H, d, J = 6.0 Hz, ^{ae}CHO*H'*), 4.72 (1H, t, J = 5.6 Hz, $^{ae}CH_2OH$), 4.63 (1H, t, J = 5.6 Hz, $^{ae}CH_2OH'$); 5.09 (1H, d, J = 5.2 Hz, $^{aa}CH_2OH$), 4.68 (1H, t, J = 5.6 Hz, $^{aa}CH_2OH$); 4.84 (0.23H, d, J = 4.8 Hz, ^{ee}CHO*H*), 4.60 (0.23H, t, J = 5.6 Hz, $^{ee}CH_2OH$), 3.70–1.60 (16H, m, $^{ae,aa,ee}CH_2CHOHCH_2OH$). Compared with traditional materials, it had the characteristics of low cytotoxicity, high biocompatibility, excellent bioavailability, and low cost [32,38]. The Mb assay represents the principal method for determining the CO liberated from CO-releasing molecules [33]. TG-Fe CORMs released free CO into solution, it will convert deoxy-Mb to Mb-CO. This conversion could be detected by observing the change in the Q-bands of the heme group in both deoxy-Mb and Mb-CO by UV–vis spectroscopic analysis (Fig. 1A). Subsequently, our findings revealed that the CO could be ingested by macrophages. We used the fluorescent probe for CO detection in living cells. Different concentrations of TG-Fe CORMs were then added to the probe solutions. Experiment showed that the reactions of probe after addition of TG-Fe CORMs (200 and 400 μg/mL) all performed smoothly, generating dose dependent fluorescence enhancement (Fig. 1B). In addition, RAW 264.7 cells were treated with different concentrations of TG-Fe CORMs for 48 h, respectively. MTT assay showed dose dependent in cell survival rate (Fig. 1C). TG-Fe CORMs could effectively maintain the maximum activity and proliferation of RAW 264.7 cells at a concentration of 200 μg/mL. These results showed that TG-Fe CORMs could effectively release CO molecules, which could be ingested by RAW 264.7 macrophages.

Numerous studies emphasized that the large accumulation of M2 macrophages on the earlier stage, could enhanced bone formation and wound healing [39], suggesting that effective manipulation of macrophage phenotype towards M2 was critical for bone formation. To investigate the effect of CO on M2 macrophage polarization *in vitro*, RAW 264.7 cells were treated with different concentration of TG-Fe CORMs for 48 h respectively. In this study, iNOS-PE and TNF-α were served as M1 macrophage markers, while CD206-APC and Arg-1 were served as M2 macrophage markers. 100 ng/mL of LPS to produce M1 macrophages (LPS-M1) and 20 ng/mL of IL-4 produce M2 macrophages (IL-4-M2). They served as negative group and positive group respectively. To determine optimum concentration of TG-Fe CORMs for macrophage polarization from M0 to M2, RAW 264.7 cells were subjected to indicated concentration (50, 100, 200 μg/mL) for 48 h. As shown in Fig. S2 (Supporting information), the data from flow cytometry indicated that CO treatment caused a switch of phenotypes from M0 toward M2 in a dose-dependent manner as demonstrated in a higher percent of CD206-APC (Fig. S2A). Fluorescence double-label flow cytometry revealed that CO treatment effectively modulated M0 macrophages into M2 phenotype, as evidenced by high expression of M2 markers (CD206-APC) and low expression of M1 marker (iNOS-PE) (Fig. S2B). The expression of mRNAs also showed the same phenotype transition trend. CO treatments promoted M2 macrophage polarization, upregulating CD206 and Arg-1 mRNA while downregulating iNOS and TNF-α mRNA (Fig. S2C). Correspondingly, at the protein level, CO treatments significantly increased Arg-1 secretion while reducing TNF-α secretion (Fig. S2D). The above results indicated that CO effectively promoted M2 phenotype macrophages polarization (CO-M2 macrophages).

It was reported that M2 macrophages could promoted the osteogenic differentiation *via* paracrine secreted cytokines [40]. To



Scheme 1. Schematic illustration of preparation and therapeutic mechanism of CO-M2-Exo. CO-M2 Exosomes transport miRNA-21 into osteoblast cells and promote high expression of Lhx8 in osteoblasts, which then promotes osteogenic differentiation and ultimately leads to new bone formation.

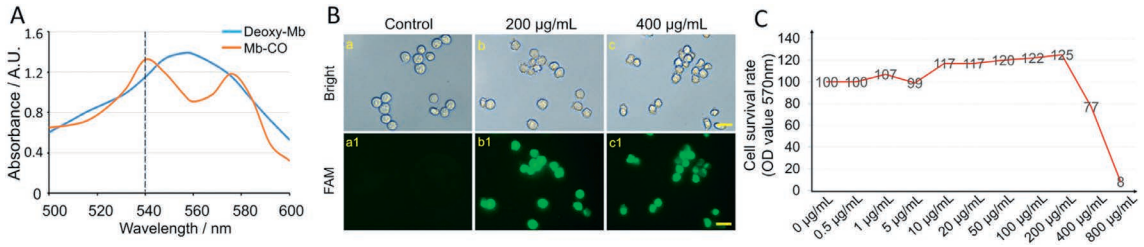


Fig. 1. CO could be released from TG -Fe CORMs and taken up by RAW 264.7 macrophages. (A) The Mb assay determined the CO liberated from TG-Fe CORMs. (B) Fluorescent imaging of CO in RAW 264.7 cells by the CO-tracking probe system (CO-probe-PdCl2). Top row a–c: bright field images. Bottom row a1–c1: fluorescent images of a–c, respectively, with excitation wavelength at 450–480 nm. a, a1: The cells were incubated with probe and PdCl2 (1 μmol/L each) for 30 min; b, b1, and c, c1: cells were pre-incubated with 200 and 400 μg/mL of CO-releasing molecules for 30 min, then with probe and PdCl2 (1 μmol/L each) for 30 min, respectively. Scale bar: 20 μm. (C) MTT assay showed the effect of different concentrations of TG-Fe CORMs on RAW 264.7 cell viability.

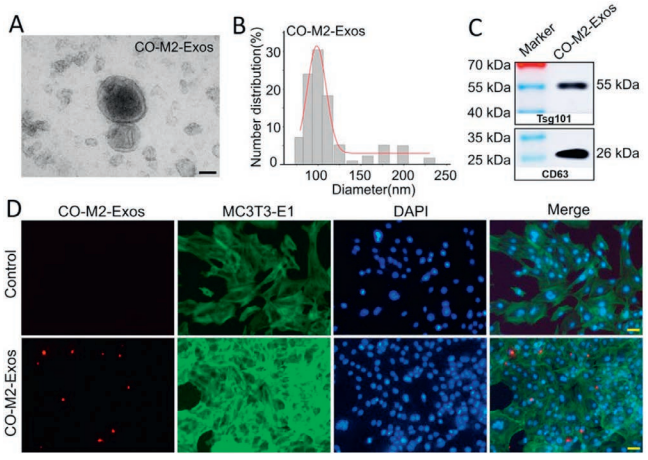


Fig. 2. Characterization of isolated CO-M2-Exos. (A) Representative scanning electron microscopy images of CO-M2-Exos. Scale bar: 50 nm. (B) Particle size distribution of CO-M2-Exos were investigated by dynamic light scattering (DLS) analysis. (C) WB analysis revealed the exosomal markers Tsg101 and CD63 were enriched in CO-M2-Exos. (D) Confocal microscopy images of Dil-labeled CO-M2-Exos (red) uptaken by MC3T3-E1 cells. The cell nuclei were stained with 4′,6-diamidino-2-phenylindole (DAPI, blue). The F-actin was stained with Actin-Tracker Green-488 (green). Scale bar: 100 μm.

analyze the effect of CO-M2 macrophages on the osteogenic ability of osteoblasts, the supernatant of CO-M2 macrophages were separately collected and directly cocultured with MC3T3-E1 cells in osteogenic induction medium for 7 or 28 days. As shown in Fig. S3 (Supporting information), CO pretreated-macrophages medium treatment group exhibited the increase in mineral deposition and osteogenic capability, which was consistent with the results of M2-type macrophages obtained by IL-4 treatment. These results showed that CO-M2 macrophages promoted osteogenic differentiation *via* paracrine signaling.

Exosomes, with a size typically between 30 nm and 150 nm, are cell-derived vesicles that play a pivotal role in mediating paracrine signaling [41]. To determine the feature of CO-M2-Exos, we purified and collected the exosomes from the exosomes-free culture supernatants of CO-M2 macrophages by ultracentrifugation. As shown in Fig. 2A, the morphology of CO-M2-Exos under Scanning electron microscopy was round or round-like vesicle. They were measured to be 50–125 nm in diameter under dynamic light scattering analysis (Fig. 2B). Western blot (WB) further showed the vesicles expressed the exosomal markers: CD63 and Tsg101 (Fig. 2C). And then, our findings revealed that the CO-M2-Exos could be endocytosed by MC3T3-E1 and the fluorescent dye Dil-labeled CO-M2-Exos were localized in the cytosol (Fig. 2D).

To analyze the effect of CO-M2-Exos cocultured with MC3T3-E1 cells on the osteogenic ability, MC3T3-E1 cells were treated with an equal volume of phosphate-buffered saline (PBS), 50 μg/mL CO-M2-Exos, or 100 μg/mL CO-M2-Exos which released into osteogenic induction medium respectively *in vitro*. Gene expression and protein levels of Alp, Runx2 and Osterix were assessed 48 h after seeding. As shown in Fig. S4 (Supporting information), as compared with the control group, the expression levels of these genes were significantly upregulated in the CO-M2-Exos group in a concentration-dependent manner (Fig. S4A). Moreover, matrix mineralization was assessed to further analyze the impact of CO-M2-Exos on osteogenesis. As shown in Fig. S4B, Alp staining and the alizarin red staining were assessed on days 7 and 28, respectively, which revealing enhanced osteogenic capability and matrix mineralization in the CO-M2-Exos groups, compared to the control group. These results indicated that CO-M2-Exos promoted osteogenic differentiation of MC3T3-E1 *in vitro*. Encouraged by *in vitro* results, we further studied the impact of CO-M2-Exos on promoting bone healing in rat models. After the 5 mm skull bone defect model was built, the local defect site was injected an equal volume of PBS, 50 μg/mL CO-M2-Exos, or 100 μg/mL CO-M2-Exos respectively (Fig. S4D). After 8 weeks of treatment, the calvarial defect specimens were harvested for micro-CT imaging and tissue staining. Compared with control group, CO-M2-Exos treatment showed more pronounce bone regeneration and healing effects. Hematoxylin and eosin (H&E) and Masson's staining results also revealed similar results as micro-computed tomography (micro-CT) examinations (Fig. S4C). And, CO-M2-Exos group could maximize the value of bone volume (Fig. S4E). These results indicated that CO-M2-Exos promoted bone regeneration *in vivo*. The experiment was approved by the Ethics Committee of School and Hospital of Stomatology, Cheeloo College of Medicine, Shandong University. All experimental conducted in accordance with the Division of Laboratory Animal Medicine guidelines. Animal experiments were approved by the Committee on the Ethics of Animal Experiments of Shandong University (No. 20211213, approval date 30 December 2021).

Exosomes play a critical role in intercellular communication by transferring bioactive molecules between cells, such as lipids, proteins, and genetic information [42,43]. miRNAs are the most numerous cargo molecules in the exosome [44]. Growing evidences indicate that miRNA delivery plays a crucial role in improving the therapeutic potential of exosomes in various disease models [45]. To investigate how CO-M2-Exos exerted osteoprotective effect by modulating osteoblastic osteogenesis, we sequenced and analyzed the microRNA of exosomes from M0 and CO-M2 macrophages culture supernatants and then miRNA-21 was found to be expressed significantly higher in CO-M2-Exos compared with M0-Exos (Fig. 3A). After that, reverse transcription quantitative polymerase chain reaction (RT-qPCR) results also revealed similar results as microRNA sequencing analysis (Fig. 3B). Next, we isolated exosomes from miRNA-21inhibitor-treated CO-M2 macrophages (CO-M2-INH-Exos) and untreated CO-M2

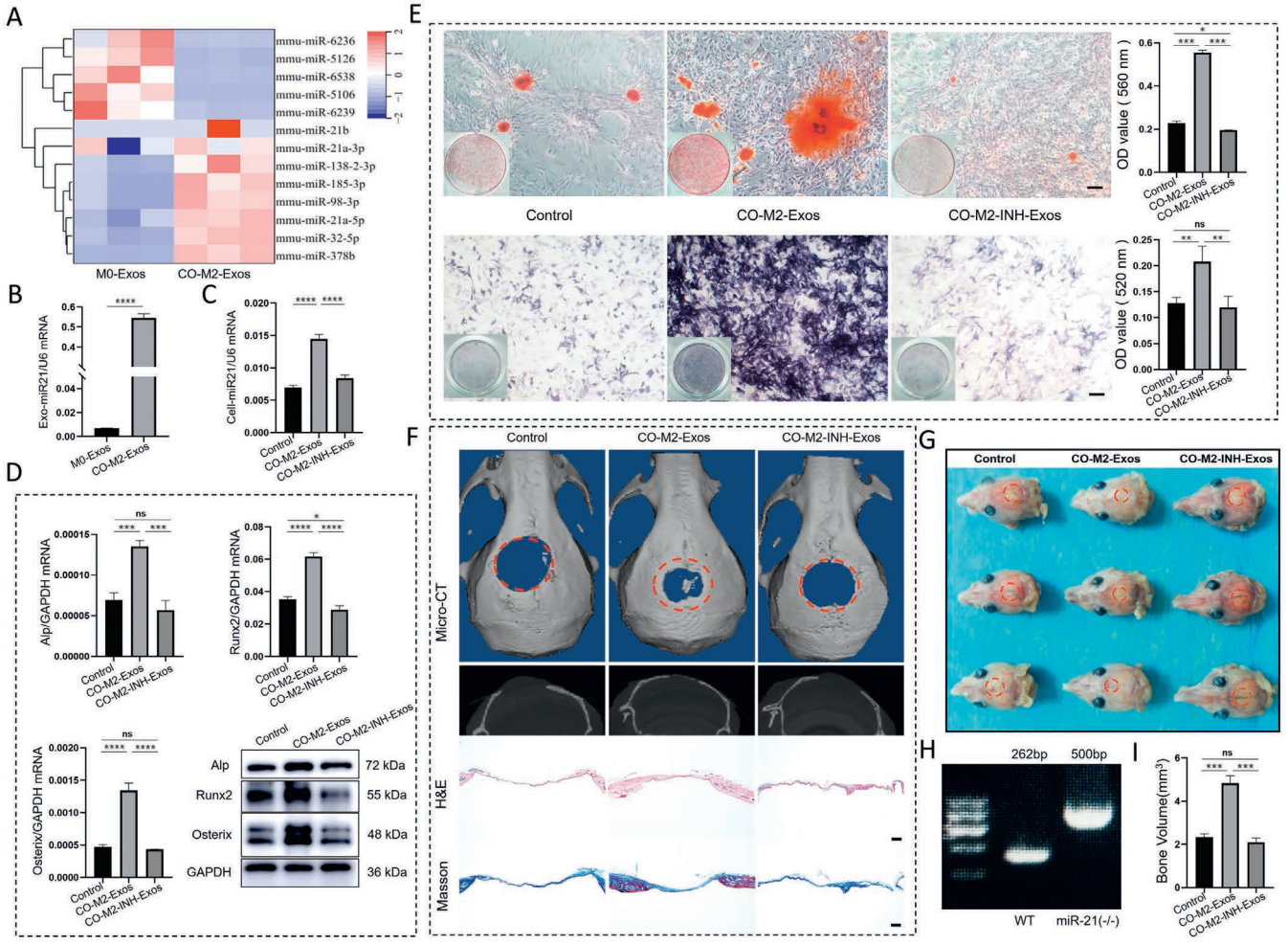


Fig. 3. CO-M2-Exosomal miRNA-21 promoted osteogenesis *in vitro* and *vivo*. (A) Heat map analysis of exosomes from CO-M2 and M0 macrophages. (B) The expression levels of miR-21 mRNAs in exosomes derived from CO-M2 and M0 macrophages were quantified using RT-qPCR. (C) The effect of CO-M2-Exosomal miRNA-21 on the expression level of miRNA-21 in MC3T3-E1 cells was assessed by RT-qPCR. (D) The effect of CO-M2-Exosomal miRNA-21 on the expression of osteogenic-related genes in MC3T3-E1 cells, as assessed by RT-qPCR and WB. (E) Alizarin red-mediated calcium staining and Alp staining in MC3T3-E1 cells after different treatments, as well as quantitative analysis. Scale bar: 100 μm. (F) Micro-CT 3D reconstruction of cranial defect sites in miRNA-21-deficient mice, Hematoxylin and eosin staining, and Masson staining for the evaluation of bone regeneration. Scale bar: 200 μm. (G) Specimen image of miRNA-21-deficient mice after surgery. (H) Agarose gel electrophoresis analysis demonstrated miRNA-21 was knocked out successfully in gene deficient mice. (I) New bone volume quantitative analysis of bone healing effect after different treatments. Data are presented by mean ± SD ($n = 3$). $^{*}P < 0.05$, $^{**}P < 0.01$, $^{***}P < 0.001$, $^{****}P < 0.0001$. ns, no significance. GAPDH, glyceraldehyde-3-phosphate dehydrogenase. U6: U6 small nuclear RNA.

macrophages, then co-cultured them with MC3T3-E1 cells for 48 h. The miRNA-21 expression level of MC3T3-E1 cells was analyzed by RT-qPCR. Results showed that miRNA-21 expression was significantly higher in the CO-M2-Exos group than in the Control and CO-M2-INH-Exos groups (Fig. 3C). These results suggested that CO-M2-Exos directly delivered exosomal miRNA-21 to MC3T3-E1 cells, thereby upregulating miRNA-21 expression. Subsequently, to investigate the role of CO-M2-Exos in regulating MC3T3-E1 cell differentiation through miRNA-21, cells were treated with equal volumes of PBS (control), CO-M2-Exos, or CO-M2-INH-Exos in osteoinductive medium. After 48 h, gene expression and protein levels of Alp, Runx2 and Osterix were assessed. Compared with the control group, mRNA and protein expression levels of these osteogenic markers were significantly upregulated in the CO-M2-Exos group, while no significant changes were observed in the CO-M2-INH-Exos group (Fig. 3D). We further analyzed the effect of CO-M2-Exosomal miRNA-21 on osteoblast differentiation using alizarin red staining and Alp staining. The results demonstrated that CO-M2-Exosomal miRNA-21 enhanced osteogenic capacity and matrix mineralization in MC3T3-E1 cells (Fig. 3E). These results confirmed that CO-M2-Exosomal miRNA-21 played a crucial role in regulating osteogenic differentiation of MC3T3-E1 cells *in vitro*.

To further investigate the effect of CO-M2-Exosomal miRNA-21 on bone regeneration *in vivo*, we established skull bone defects in miRNA-21-deficient mice (Figs. 3G and H). After 12 weeks of treatment, bone regeneration was evaluated by micro-CT imaging and histological staining (Fig. 3F). The results showed that the CO-M2-Exos group clearly taken place bone regeneration and remodeling. However, when miRNA-21 was inhibited in CO-M2-Exos, skeletogenesis was substantially reduced in bone defect compared with CO-M2-Exos group, indicating a critical role of CO-M2-Exosomal miRNA-21 in bone regeneration. H&E and Masson's staining further confirmed the pronounced bone regeneration mediated by CO-M2-Exosomal miRNA-21 compared to control and CO-M2-INH-Exos treatments. Bone volume analysis also corroborated these findings (Fig. 3I). These results collectively demonstrated that CO-M2-Exosomal miRNA-21 does play a crucial role in regulating bone regeneration *in vivo*.

To investigate the mechanism by which CO-M2-Exosomal miRNA-21 regulates osteogenic differentiation in MC3T3-E1 cells, we performed mRNA sequencing analysis comparing MC3T3-E1 cells with and without exogenous miRNA-21 treatment. The analysis revealed significantly higher expression of Lhx8 mRNA (Fig. 4A), which was supported by our validation with RT-qPCR and WB

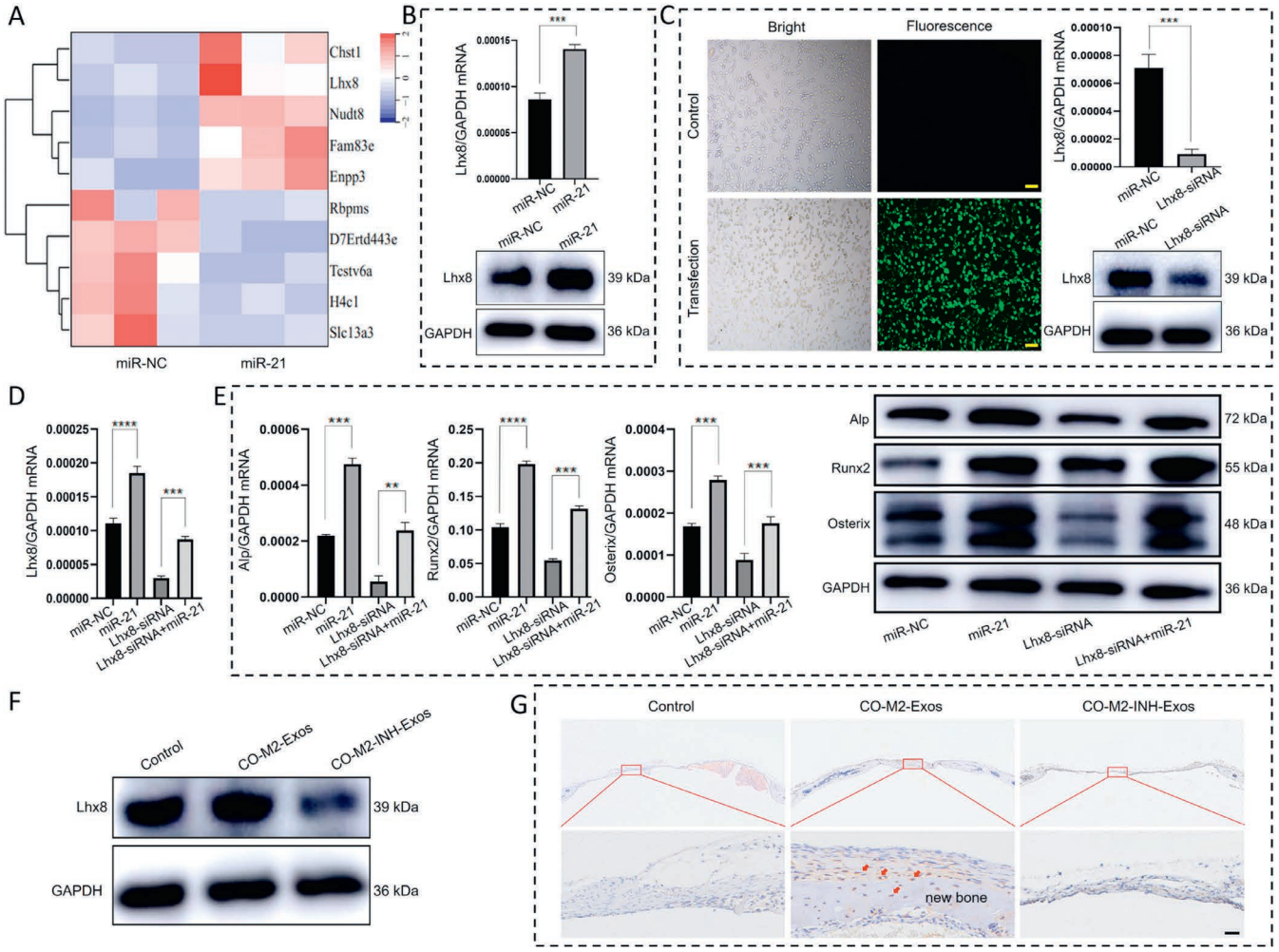


Fig. 4. CO-M2-Exosomal miRNA-21 regulated osteoblastic differentiation of MC3T3-E1 cells *via* Lhx8. (A) Heatmap analysis of gene expression in MC3T3-E1 cells after miRNA-21 transfection. (B) The expression levels of Lhx8 mRNA and protein in miRNA-21-treated MC3T3-E1 cells, as assessed by RT-qPCR and WB. (C) Establishment of MC3T3-E1 cells with low expression of Lhx8. Observation of transfection effect under fluorescence microscopy. Positive transfected cells show green fluorescence. Scale bar: 200 μm. The expression levels of Lhx8 mRNA and protein in Lhx8 siRNA-treated MC3T3-E1 cells, as assessed by RT-qPCR and WB. (D) The mRNA expression level of Lhx8 gene in Lhx8 siRNA-treated MC3T3-E1 cells after miRNA-21 treatment, as assessed by RT-qPCR. (E) The mRNA and protein expression levels of osteogenesis-related genes in Lhx8 siRNA-treated MC3T3-E1 cells after miRNA21 treatment, as assessed by RT-qPCR and WB. (F) The expression levels of Lhx8 protein in CO-M2-Exos-treated MC3T3-E1 cells, as assessed by WB. (G) The expression levels of Lhx8 and new bone formation in CO-M2-Exos-treated miRNA-21-deficient mice cranial defect model. The red arrow indicated positive expression of Lhx8. Scale bar: 20 μm. Data are presented by mean ± SD ($n = 3$). $^{*}P < 0.05$, $^{**}P < 0.01$, $^{***}P < 0.001$, $^{****}P < 0.0001$.

(Fig. 4B). We then established Lhx8-knockdown MC3T3-E1 cells (Fig. 4C). Following 48 h miRNA-21 treatment, we quantified the expression level of osteogenic markers (Alp, Runx2, and Osterix) using RT-qPCR and WB. Both mRNA and protein levels were significantly downregulated in the Lhx8-siRNA group, but were rescued by adding miRNA-21 in the Lhx8-siRNA+miR-21 group (Fig. 4E). Similarly, Lhx8 mRNA expression showed comparable rescue effects (Fig. 4D). Furthermore, we confirmed that CO-M2-Exos could promote an increase in protein expression levels of Lhx8 in MC3T3-E1 cells (Fig. 4F). And, *in vivo* experiments, CO-M2-Exos promoted Lhx8 expression and new bone formation in miRNA-21-deficient mice cranial defect model (Fig. 4G). These findings demonstrated that CO-M2-Exosomal miRNA-21 could advance the Lhx8 expression, thereby regulating bone regeneration. The LIM-homeobox 8 (Lhx8), which is also known as L3 and Lhx7, is a remarkably conserved transcriptional factor of the LIM-homeobox family among species. Research has shown that Lhx8 is abundantly expressed during craniofacial bone development [46]. In addition, Lhx8 plays a critical role in balancing proliferation and osteogenic differentiation in BMSCs [47,48]. During the osteogenic differentiation of BMSCs, the expression levels of Lhx8 regulate the new bone formation *in vitro* and *in vivo* [49], and is closely related to the expression of osteogenic related factor BMP-2 [50,51]. However, the exact regulatory mechanism of Lhx8 in osteogenic differentiation yet to be elucidated. Our results revealed that the exosomal miRNA-21 could facilitate the expression of Lhx8 in osteoblasts, thus to promote osteogenic differentiation of osteoblasts and bone regeneration. To our knowledge, this is the first report on the relationship between the miRNA-21/Lhx8 signaling axis and osteogenic differentiation, which will provide a theoretical basis for the study of osteogenic differentiation mechanism in osteoblasts.

Exosomes, as a specialized subgroup of extracellular vesicles, demonstrate immense potential for alveolar bone regeneration [52], providing a transformative alternative to traditional treatments for alveolar bone defects [45]. In this study, we report the first-ever use of a hydrophilic and stable TG-Fe CORMs to engineer M2 macrophage-derived exosomes, marking a groundbreaking advancement in regenerative medicine. This innovative method enabled precise and controlled CO delivery, effectively polarizing M2 macrophages and producing exosomes with enhanced regenerative capabilities. These CO-engineered exosomes significantly induced osteogenic differentiation of osteoblasts and promoted bone regen-

eration calvarial defect models. By creating a favorable microenvironment through CO modulation, we optimized exosome composition and functionality. This pioneering strategy establishes a scalable, cell-free therapeutic approach, leveraging advanced CO drug delivery systems to ensure safety, efficiency, and clinical applicability in alveolar bone regeneration and immune modulation.

Declaration of competing interest

The authors declare that they have no known competing financial interests or personal relationships that could have appeared to influence the work reported in this paper.

CRediT authorship contribution statement

Zhiyuan Shen: Writing – original draft, Visualization, Validation, Software, Resources, Project administration, Methodology, Investigation, Formal analysis, Data curation, Conceptualization. **Tianyi Li:** Methodology, Investigation, Formal analysis, Data curation. **Zijie Zhang:** Visualization, Validation, Software. **Jiani Liu:** Project administration, Methodology, Investigation, Data curation. **Jun Wu:** Visualization, Supervision, Resources, Conceptualization. **Qing Li:** Writing – review & editing, Supervision, Funding acquisition, Conceptualization. **Fulan Wei:** Writing – review & editing, Supervision, Funding acquisition, Conceptualization.

Acknowledgments

This work was supported by the National Natural Science Foundation of China (Nos. 818027091, 82470951, 82071080); the Fundamental Research Funds for the Central Universities (No. 2022JC017); Academician Laboratory of Immune and Oral Development & Regeneration, Dalian Medical University (No. 2021002); the Shandong Provincial Natural Science Foundation, China (No. ZR2023MH230); the Future Young Scholars Program of Shandong University.

Supplementary materials

Supplementary material associated with this article can be found, in the online version, at doi:10.1016/j.cclet.2025.111641.

References

[1] T. Li, X. Zeng, S. Zou, Y. Xu, P. Duan, Biomed. Mater. 18 (2023) 052004.
[2] S. Tsuchida, T. Nakayama, Biomedicines 11 (2023) 843.
[3] N. Mardas, N. Macbeth, N. Donos, R.E. Jung, A.N. Zuercher, Periodontol. 2000 93 (2023) 289–308.
[4] E. Couso-Queiruga, S. Stuhr, M. Tattan, L. Chambrone, G. Avila-Ortiz, J. Clin. Periodontol. 48 (2021) 126–144.
[5] J. Lu, Z. Wang, H. Zhang, et al., Tissue Eng. Part B: Rev. 28 (2022) 35–51.
[6] G. Jiang, S. Li, K. Yu, et al., Acta Biomater. 128 (2021) 150–162.
[7] L.A. Mills, S.A. Aitken, A. Simpson, Acta Orthop. 88 (2017) 434–439.
[8] J. Lyu, H. Chen, J. Luo, et al., Int. J. Biol. Macromol. 260 (2024) 129454.
[9] S. Ozzo, M. Kheirallah, BMC. Oral Health 24 (2024) 1040.
[10] L. Tavelli, S. Barootchi, G. Rasperini, W.V. Giannobile, Periodontol. 2000 91 (2023) 217–269.
[11] L. Xiao, H. Liu, S. Wu, et al., Adv. Fiber Mater. 7 (2024) 72–92.
[12] Ž.Perić Kačarević, P. Rider, S. Alkildani, et al., Int. J. Artif. Organs 43 (2020) 69–86.
[13] Q. Hu, C.J. Lyon, J.K. Fletcher, et al., Acta Pharm. Sin. B 11 (2021) 1493–1512.
[14] A.Y. Mun, K. Akiyama, Z. Wang, et al., JBMR Plus 8 (2024) ziae085.
[15] Y. Huang, X. Zhai, T. Ma, et al., Adv. Mater. 35 (2023) e2300313.
[16] H. Huang, L. Xiao, L. Fang, et al., ACS Nano 19 (2025) 8667–8691.
[17] S.M. Kronstadt, D.B. Patel, L.J. Born, et al., Adv. Healthc. Mater. 12 (2023) e2300584.
[18] R. Jeske, C. Liu, L. Duke, et al., Bioact. Mater. 25 (2023) 732–747.
[19] X. Huang, Y. Deng, J. Xiao, et al., Bioact. Mater. 32 (2024) 473–487.
[20] Y. Liu, S. Lin, Z. Xu, et al., Adv. Sci. 11 (2024) e2309491.
[21] Y.K. Zhou, C.S. Han, Z.L. Zhu, et al., Bioact. Mater. 31 (2024) 192–205.
[22] S.V. Krylova, D. Feng, Int. J. Mol. Sci. 24 (2023) 1337.
[23] W. Huang, Q. Guo, H. Wu, et al., ACS Nano 19 (2025) 14467–14483.
[24] D.M. Pegtel, S.J. Gould, Annu. Rev. Biochem. 88 (2019) 487–514.
[25] W. Li, Z. Yu, Z. Wu, J. Jia, G. Chen, Translat. Dent. Res. 1 (2025) 100004.
[26] F. Meng, G. Wang, F. Zhou, et al., Compos. B Eng. 276 (2024) 111358.
[27] X. Chen, Z. Wan, L. Yang, et al., J. Nanobiotechnology 20 (2022) 110.
[28] S.J. Zhao, F.Q. Kong, J. Jie, et al., Theranostics 10 (2020) 17–35.
[29] P.P. Oza, K. Kashfi, Pharmacol. Ther. 249 (2023) 108502.
[30] Y. Yuan, H. Zhang, H. Huang, J. Periodontal Res. 56 (2021) 219–225.
[31] M. Zhou, G. Li, J. Yu, et al., Bioact. Mater. 40 (2024) 318–333.
[32] C. Gao, X. Liang, Z. Guo, et al., ACS Omega 3 (2018) 2683–2689.
[33] A.J. Atkin, J.M. Lynam, B.E. Moulton, et al., Dalton. Trans. 40 (2011) 5755–5761.
[34] S. Ye, N. Jin, N. Liu, et al., Biomater. Sci. 12 (2024) 3273–3292.
[35] S.W. Ryter, L.E. Otterbein, Bioessays 26 (2004) 270–280.
[36] S.W. Ryter, J. Alam, A.M. Choi, Physiol. Rev. 86 (2006) 583–650.
[37] Z. Yuan, L.K. De La Cruz, X. Yang, B. Wang, Pharmacol. Rev. 74 (2022) 823–873.
[38] L. Long, X. Jiang, X. Wang, Z. Xiao, X. Liu, Dalton. Trans. 42 (2013) 15663–15669.
[39] R. Toita, J.H. Kang, A. Tsuchiya, Acta Biomater. 154 (2022) 583–596.
[40] B. Li, F. Liu, J. Ye, et al., Small 18 (2022) e2202691.
[41] Y. Xu, L. Ma, Y. Wang, C. Shi, Chin. Chem. Lett. 36 (2025) 109766.
[42] Y. Zhang, H. Liu, X. Liu, et al., Aging 12 (2020) 6067–6088.
[43] Y. Zhuang, S. Jiang, X. Deng, et al., Sci. Adv. 10 (2024) eadl0372.
[44] R. Madhyastha, H. Madhyastha, Q.I. Nurrahmah, et al., Inflammation 44 (2021) 1274–1287.
[45] Y. Lu, Z. Mai, L. Cui, X. Zhao, Stem Cell Res. Ther. 14 (2023) 55.
[46] C. Zhou, G. Yang, M. Chen, et al., FASEB J. 29 (2015) 4083–4091.
[47] W. Wang, D. Huang, J. Ren, et al., Theranostics 9 (2019) 8196–8205.
[48] Y. Du, H. Zhong, C. Yu, et al., Heliyon 9 (2023) e19878.
[49] D. Huang, R. Li, J. Ren, et al., Stem Cell Res. Ther. 12 (2021) 339.
[50] C. Zhou, D. Chen, J. Ren, et al., J. Cell Mol. Med. 25 (2021) 3051–3062.
[51] Y. Liu, H. Wang, H. Dou, et al., J. Tissue Eng. 11 (2020) 2041731420930379.
[52] F. Lei, M. Li, T. Lin, et al., Acta Biomater. 141 (2022) 333–343.